747-793, 1993.
24. Kriss JP, Pleshakov V, Rosenblum AL, Holderness M, Sharp G, Utiger R. Studies on the pathogenesis of the ophthalmopathy of Graves' disease. J Clin Endocrinol Metab **27**: 582-593, 1967.
25. Solomon DH, Chopra IJ, Chopra U, Smith FJ. Identification of subgroups of euthyroid Graves's ophthalmopathy. N Engl J Med **296**: 181-186, 1977.
26. Marcocci C, Bruno-Bossio G, Manetti L, et al. The course of Graves' ophthalmopathy is not influenced by near total thyroidectomy: a case-control study. Clin Endocrinol (Oxf) **51**: 503-508, 1999.
27. Kim JM, LaBree L, Levin L, Feldon SE. The relation of Graves' ophthalmopathy to circulating thyroid hormone status. Br J Ophthalmol **88**: 72-74, 2004.
28. Perros P, Crombie AL, Matthews JN, Kendall-Taylor P. Age and gender influence the severity of thyroid-associated ophthalmopathy: a study of 101 patients attending a combined thyroid-eye clinic. Clin Endocrinol (Oxf) **38**: 367-372, 1993.
29. Kozaki A, Inoue R, Komoto N, et al. Proptosis in dysthyroid ophthalmopathy: a case series of 10,931 Japanese cases. Optom Vis Sci **87**: 200-204, 2010.
30. Forbes G, Gorman CA, Brennan MD, Gehring DG, Ilstrup DM, Earnest F 4th. Ophthalmopathy of Graves' disease: computerized volume measurements of the orbital fat and muscle. AJNR Am J Neuroradiol **7**: 651-656, 1986.
31. Abraham-Nordling M, Byström K, Törring O, et al. Incidence of hyperthyroidism in Sweden. Eur J Endocrinol **165**: 899-905, 2011.
32. Manji N, Carr-Smith JD, Boelaert K, et al. Influences of age, gender, smoking, and family history on autoimmune thyroid disease phenotype. J Clin Endocrinol Metab **91**: 4873-4880, 2006.
33. Bartalena L, Wiersinga WM, Pinchera A. Graves' ophthalmopathy: state of the art and perspectives. J Endocrinol Invest **27**: 295-301, 2004.
34. Krassas GE. Childhood Graves' orbitopathy. In: Graves' Orbitopathy: A Multidisciplinary Approach-Questions and Answers. 2nd ed. Wiersinga WM, Kahaly GJ, Eds. Karger, Basel, 2010: 239-247.
35. Young LA. Dysthyroid ophthalmopathy in children. J Pediatr Ophthalmol Strabismus **16**: 105-107, 1979.
36. Uretsky SH, Kennerdell JS, Gutai JP. Graves' ophthalmopathy in childhood and adolescence. Arch Ophthalmol **98**: 1963-1964, 1980.
37. Grüters A. Ocular manifestations in children and adolescents with thyrotoxicosis. Exp Clin Endocrinol Diabetes **107** (Suppl 5): S172-S174, 1999.
38. Chan W, Wong GW, Fan DS, Cheng AC, Lam DS, Ng JS. Ophthalmopathy in childhood Graves' disease. Br J Ophthalmol **86**: 740-742, 2002.
39. Durairaj VD, Bartley GB, Garrity JA. Clinical features and treatment of Graves' ophthalmopathy in pediatric patients. Ophthal Plast Reconstr Surg **22**: 7-12, 2006.
40. Blake CR, Lai WW, Edward DP. Racial and ethnic differences in ocular anatomy. Int Ophthalmol Clin **43**: 9-25, 2003.
41. Chng CL, Seah LL, Khoo DHC. Ethnic differences in the clinical presentation of Graves' ophthalmopathy. Best Pract Res Clin Endocrinol Metab **262**: 249-258, 2012.
42. de Juan E Jr, Hurley DP, Sapira JD. Racial differences in normal values of proptosis. Arch Intern Med **140**: 1230-1231, 1980.
43. Tsai CC, Kau HC, Kao SC, Hsu WM. Exophthalmos of patients with Graves' disease in Chinese of Taiwan. Eye (Lond) **20**: 569-573, 2006.
44. Amino N, Yuasa T, Yabu Y, Miyai K, Kumahara Y. Exophthalmos in autoimmune thyroid disease. J Clin Endocrinol Metab **51**: 1232-1234, 1980.
45. Kim IT, Choi JB. Normal range of exophthalmos values on orbit computerized tomography in Koreans. Ophthalmologica **215**: 156-162, 2001.
46. Rootman J. Aspects of current management of thyroid orbitopathy in Asians. Asia Pacific J Ophthalmol **10**: 2-6, 1998.
47. Daumerie C. Epidemiology in Graves' orbitopathy. In: Graves' Orbitopathy: A Multidisciplinary Approach-Questions and Answers. 2nd ed. Wiersinga WM, Kahaly GJ, Eds. Karger, Basel, 2010: 33-39.
48. Hiromatsu Y, Kojima K, Ishisaka N, et al. Role of magnetic resonance imaging in thyroid-associated ophthalmopathy: its predictive value for therapeutic outcome of immunosuppressive therapy. Thyroid **2**: 299-305, 1992.
49. Kirsch E, Hammer B, von Arx G. Graves' orbitopathy: current imaging procedures. Swiss Med Wkly **139**: 618-623, 2009.
50. Bartalena L, Baldeschi L, Dickinson AJ, et al. Consensus statement of the European group on Graves' orbitopathy (EUGOGO) on management of Graves' orbitopathy. Thyroid **18**: 333-346, 2008.
51. Tachibana S, Murakami T, Noguchi H, et al. Orbital magnetic resonance imaging combined with clinical activity score can improve the sensitivity of detection of disease activity and prediction of response to immunosuppressive therapy for Graves' ophthalmopathy. Endocr J **57**: 853-861, 2010.
52. Classification of eye changes of Graves' disease. Thyroid **2**: 235-236, 1992.
53. Dckinson AJ. Clinical manifestations. In: Graves' Orbitopathy: A Multidisciplinary Approach-Questions and Answers. 2nd ed. Wiersinga WM, Kahaly GJ, Eds. Karger, Basel, 2010: 1-25.
54. Villadolid MC, Yokoyama N, Izumi M, et al. Untreated Graves' disease patients without clinical ophthalmopathy demonstrate a high frequency of extraocular muscle (EOM) enlargement by magnetic resonance. J Clin Endocrinol Metab **80**: 2830-2833, 1995.
55. Enzmann DR, Donaldson SS, Kriss JP. Appearance of Graves' disease on orbital computed tomography. J Comput Assist Tomogr **3**: 815-819, 1997.
56. Gupta A, Sadeghi PB, Akpek EK. Occult thyroid eye disease in patients presenting with dry eye symptoms. Am J Ophthalmol **147**: 919-923, 2009.
57. Tellez M, Cooper J, Edmonds C. Graves' ophthalmopathy in relation to cigarette smoking and ethnic origin. Clin Endocrinol (Oxf) **36**: 291-294, 1992.
58. Krassas GE, Segni M, Wiersinga WM. Childhood Graves' ophthalmopathy: results of a European questionnaire study. Eur J Endocrinol **153**: 515-521, 2005.
59. Laurberg P, Berman DC, Bülow Pedersen I, Andersen S, Carlé A. Incidence and clinical presentation of moderate to severe Graves' orbitopathy in a Danish population before and after iodine fortification of salt. J Clin Endocrinol Metab **97**: 2325-2332, 2012.
60. Perros P, Kendall-Taylor P. Natural history of thyroid eye disease. Thyroid **8**: 423-425, 1998.
61. Weetman AP, Wiersinga WM. Current management of thyroid-associated ophthalmopathy in Europe. Results of an international survey. Clin Endocrinol (Oxf) **49**: 21-28, 1998.
62. Rundle FF, Wilson CW. Development and course of exophthalmos and ophthalmoplegia in Graves' disease with special reference to the effect of thyroidectomy. Clin Sci **5**: 177-194, 1945.
63. Rundle FF. Management of exophthalmos and related ocular changes in Graves' disease. Metabolism **6**: 36-48, 1957.
64. Wiersinga WM. Advances in medical therapy of thyroid-associated ophthalmopathy. Orbit **15**: 177-186, 1996.
65. Streeten DH, Anderson GH Jr, Reed GF, Woo P. Prevalence, natural history and surgical treatment of exophthalmos. Clin Endocrinol (Oxf) **27**: 125-133, 1987.
66. Perros P, Crombie AL, Kendall-Taylor P. Natural history of thyroid associated ophthalmopathy. Clin Endocrinol (Oxf) **42**: 45-50, 1995.
67. Noth D, Gebauer M, Müller B, Bürgi U, Diem P. Graves' ophthal-

mopathy: natural history and treatment outcomes. Swiss Med Wkly **131**: 603-639, 2001.

68. Tanda ML, Piantanida E, Liparulo L, et al. Prevalence and natural history of Graves' orbitopathy in a large series of patients with newly diagnosed Graves' hyperthyroidism seen at a single center. J Clin Endocrinol Metab **98**: 1443-1449, 2013.

69. Tallstedt L, Lundell G, Tørring O, et al. Occurrence of ophthalmopathy after treatment for Graves' hyperthyroidism. The Thyroid Study Group. N Engl J Med **326**: 1733-1738, 1992.

70. Bartalena L, Marcocci C, Bogazzi F, et al. Relation between therapy for hyperthyroidism and the course of Graves' ophthalmopathy. N Engl J Med **338**: 73-78, 1998.

71. Tallstedt L, Lundell G, Blomgren H, Bring J. Does early administration of thyroxine reduce the development of Graves' ophthalmopathy after radioiodine treatment? Eur J Endocrinol **130**: 494-497, 1994.

72. Perros P, Kendall-Taylor P, Neoh C, Frewin S, Dickinson J. A prospective study of the effects of radioiodine therapy for hyperthyroidism in patients with minimally active Graves' ophthalmopathy. J Clin Endocrinol Metab **90**: 5321-5323, 2005.

73. Träisk F, Tallstedt L, Abraham-Nordling M, et al. Thyroid-associated ophthalmopathy after treatment for Graves' hyperthyroidism with antithyroid drugs or iodine-131. J Clin Endocrinol Metab **94**: 3700-3707, 2009.

74. Bahn RS, Burch HB, Cooper DS, et al. Hyperthyroidism and other causes of thyrotoxicosis: management guidelines of the American Thyroid Association and American Association of Clinical Endocrinologists. Endocr Pract **17**: 456-520, 2011.

75. Selva D, Chen C, King G. Late reactivation of thyroid orbitopathy. Clin Experiment Ophthalmol **32**: 46-50, 2004.

76. Eckstein AK, Plicht M, Lax H, et al. Thyrotropin receptor autoantibodies are independent risk factors for Graves' ophthalmopathy and help to predict severity and outcome of the disease. J Clin Endocrinol Metab **91**: 3464-3470, 2006.

77. Kamizono S, Hiromatsu Y, Seki N, et al. A polymorphism of the 5' flanking region of tumour necrosis factor alpha gene is associated with thyroid-associated ophthalmopathy in Japanese. Clin Endocrinol (Oxf) **52**: 759-764, 2000.

78. Vestergaard P. Smoking and thyroid disorders: a meta-analysis. Eur J Endocrinol **146**: 153-161, 2002.

79. Bartalena L, Martino E, Marcocci C, et al. More on smoking habits and Graves' ophthalmopathy. J Endocrinol Invest **12**: 733-737, 1989.

80. Hegediüs L, Brix TH, Vestergaard P. Relationship between cigarette smoking and Graves' ophthalmopathy. J Endocrinol Invest **27**: 265-271, 2004.

81. Khoo DH, Ho SC, Seah LL, et al. The combination of absent thyroid peroxidase antibodies and high thyroid-stimulating immunoglobulin levels in Graves' disease identifies a group at markedly increased risk of ophthalmopathy. Thyroid **9**: 1175-1180, 1999.

82. Noh JY, Hamada N, Inoue Y, Abe Y, Ito K, Ito K. Thyroid-stimulating antibody is related to Graves' ophthalmopathy, but thyrotropin-binding inhibitor immunoglobulin is related to hyperthyroidism in patients with Graves' disease. Thyroid **10**: 809-813, 2000.

83. Goh SY, Ho SC, Seah LL, Fong KS, Khoo DH. Thyroid autoantibody profiles in ophthalmic dominant and thyroid dominant Graves' disease differ and suggest ophthalmopathy is a multiantigenic disease. Clin Endocrinol (Oxf) **60**: 600-607, 2004.

84. Lytton SD, Ponto KA, Kanitz M, Matheis N, Kohn LD, Kahaly GJ. A novel thyroid stimulating immunoglobulin bioassay is a functional indicator of activity and severity of Graves' orbitopathy. J Clin Endocrinol Metab **95**: 2123-2131, 2010.

85. Gerding MN, van der Meer JW, Broenink M, Bakker O, Wiersinga WM, Prummel MF. Association of thyrotrophin receptor antibodies with the clinical features of Graves' ophthalmopathy. Clin Endocrinol (Oxf) **52**: 267-271, 2000.

86. Kahaly GJ, Pitz S, Hommel G, Dittmar M. Randomized, single blind trial of intravenous versus oral steroid monotherapy in Graves' orbitopathy. J Clin Endocrinol Metab **90**: 5234-5240, 2005.

87. Eckstein AK, Plicht M, Lax H, et al. Clinical results of anti-inflammatory therapy in Graves' ophthalmopathy and association with thyroidal autoantibodies. Clin Endocrinol (Oxf) **61**: 612-618, 2004.

88. Acharya SH, Avenell A, Philip S, Burr J, Bevan JS, Abraham P. Radioiodine therapy (RAI) for Graves' disease (GD) and the effect on ophthalmopathy: a systematic review. Clin Endocrinol (Oxf) **69**: 943-950, 2008.

89. Laurberg P, Wallin G, Tallstedt L, Abraham-Nordling M, Lundell G, Tørring O. TSH-receptor autoimmunity in Graves' disease after therapy with anti-thyroid drugs, surgery, or radioiodine: a 5-year prospective randomized study. Eur J Endocrinol **158**: 69-75, 2008.

Endocrine Journal 2014, **61** (9), 933-939

RAPID COMMUNICATION

Nucleobindin-2 is a positive regulator for insulin-stimulated glucose transporter 4 translocation in fenofibrate treated E11 podocytes

Tsugumichi Saito[1], Eijiro Yamada[1], Shuichi Okada[1], Yoko Shimoda[1], Yuko Tagaya[1], Koshi Hashimoto[2], Tetsurou Satoh[1], Masatomo Mori[3], Junichi Okada[1], Jeffrey E. Pessin[4] and Masanobu Yamada[1]

[1] *Department of Medicine and Molecular Science, Gunma University Graduate School of Medicine, Maebashi 371-8511, Japan*
[2] *Department of Metabolic Preemptive Medicine, Graduate School of Medical and Dental Sciences, Tokyo Medical and Dental University, Tokyo 113-8510, Japan*
[3] *Kitakanto obesity and metabolic research institute, Midori 379-2311, Japan*
[4] *Departments of Medicine and Molecular Pharmacology, Albert Einstein College of Medicine, NY, USA*

Abstract. The physiology of insulin signaling under normal and disease conditions is well studied in classical insulin target tissues, but not in podocytes. To examine insulin stimulation of podocyte GLUT4 translocation, we established a protocol involving treatment with the PPARα agonist fenofibrate to induce E11 podocyte differentiation within 48 hours rather than 7-10 days, which is required for differentiation under the reported protocol. This allowed us to transiently introduce GLUT4 reporter cDNA and RNAi and thereby to examine the regulatory pathway involved. Here we demonstrate that treatment with 200μM fenofibrate for 36 hours following transfection had a dramatic effect on podocyte morphology, induced several podocyte specific protein expression markers (G protein-coupled receptor 137B, chloride intracellular channel 5, and nephrin) and resulted in insulin-stimulated GLUT4 translocation. In addition, Nucleobindin-2 was found to constitutively associate with Septin 7 (the repressor of GLUT4 translocation), and knockdown of Nucleobindin-2 was found to completely abrogate insulin-stimulated GLUT4 translocation. Together, these data suggest that Nucleobindin-2 may repress Septin7-induced inhibition of insulin-stimulated GLUT4 translocation in podocytes.

Key words: Nucleobindin-2, Podocyte, Insulin resistance, Glucose transporter 4 translocation, Insulin

NUCLEOBINDINS (Nucleobindin-1 [CALNUC, NUCB1] and Nucleobindin-2 [NEFA, NUCB2]) are a class of multi-domain Ca^{2+} binding proteins that share 62% amino acid identify [1]. The cellular localization of Nucleobindin-1 has been variously suggested to be a nuclear protein [2], secreted protein [3, 4], a resident endoplasmic reticulum protein [5] and as well as localized to the cytoplasm [6]. Similarly, Nucleobindin-2 (NEFA) was also reported as localized to the cytoplasm, on the plasma membrane, as well as being secreted in the culture medium [7].

Nucleobindin-2 contains 420 amino acids that can be further processed to generate an 82 amino terminal peptide termed Nesfatin-1. However the physiological action of Nucleobindin-2 is still poorly defined. It has been reported that Nesfatin-1 but not Nucleobindin-2 is anorexigenic as Nesfatin-1 blocked food intake whereas a Nucleobindin-2 mutant that could not be processed into Nesfatin-1 was without effect [8]. Recently Broberger *et al.* reported that Nucleobindin-2 co-localizes with insulin in rat and human pancreatic β cells [9]. Since islet Nucleobindin-2 content isolated from an animal model of type 2 diabetic rats was lower than that of non-diabetic control animal, Nucleobindin-2 was suggested to play a regulatory role in insulin secretion and as a potential contributor to diabetic pathology [9]. Recently centrally administrated Nesfatin-1 was reported to increase peripheral and hepatic insulin sensitivity by decreasing gluconeogenesis and promot-

Submitted Jul. 18, 2014; Accepted Aug. 19, 2014 as EJ14-0330
Released online in J-STAGE as advance publication Aug. 27, 2014
Correspondence to: Shuichi Okada, Department of Medicine and Molecular Science, Gunma University Graduate School of Medicine, 3-39-15 Showa-machi, Maebashi, Gunma 371-8511, Japan. E-mail: okadash@gunma-u.ac.jp

Abbreviations: Clic5, Chloride intracellular channel 5; VAMP2, Vesicle-associated membrabe protein 2; GLUT4, Glucose trasnporter 4; S.D., Standard deviation; NUCB2, Nucleobindin-2; PPAR, Peroxisome proliferator-activated receptor

ing peripheral glucose uptake *in vivo* [10]. In addition, Nesfatin-1, but not Nucleobindin-2, was reported to increase glucose uptake and GLUT4 translocation in cardiomyocytes [11].

Recently, it has been reported that insulin stimulates GLUT4 translocation of podocytes that it negatively regulated by Septin7 [12]. Disturbances of podocyte slit diaphragm structure has been defined as an important cause of proteinuria and proteinuria may directly result as a consequence of podocyte insulin resistance [13]. Thus a detailed understanding of normal and pathophysiologic insulin signaling is critical for our understanding of kidney dysfunction in diabetes and the metabolic syndrome. As the potential role of Nucleobindin-2 in podocyte biology has not been examined, we have determined that Nucleobindin-2 is a novel Septin7 binding partner and that Nucleobindin-2 negatively regulates insulin-stimulated GLUT4 translocation in podocytes.

Materials and Methods

Reagents

GPR137B, Clic5, GLUT4, Nephrin, Syntaxin4, Septin7, and Nucleobindin-2 polyclonal antibody were obtained from Sigma-Aldrich. ECL and ECL+plus Western Blotting Detection System were obtained from GE Healthcare. The anti-mouse and anti-rabbit IgG-HRP were obtained from PIERCE. Cell culture media and reagents were from Invitrogen Life Technologies. ShRNA constructs against Mus. musculus Nucleobindin-2 was purchased from OriGene. All of other chemicals used in this study were purchased from Sigma-Aldrich.

Cell culture

Studies involved use of a conditionally mouse E11 podocyte cell line with modified culture condition. Usually the podocytes were cultured in RPMI-1640 media containing 10% fetal bovine serum, 100U/mL penicillin, and 100μg/mL streptomycin and were propagated in a medium containing 10U/mL mouse interferon-γ at 33°C [12, 14]. To differentiation, cells were plated in collagen type I-coated flasks under the nonpermissive condition (37°C without interferon-γ) for 7-10 days [12, 14]. However, under these conditions, we are not able to perform the experiments combined with transient transfection by electroporation because the expressed protein will start to diminish 48 hours after the transfection [15]. We therefore established an efficient transfection methodology (approximately 70%) for the E11 podocyte cell line as previously we reported [16].

However we have to maintain the cells at 37°C and lift up the cells by trypsinization. Then we have to replate the electroporated cells in suitable plate and let the replated cells differentiate at 37°C within the next 48 hours. To explore this we tested proliferator-activated receptor-α agonist fenofibrate because previous study reported that peroxisome proliferator-activated receptor-α is renoprotective and attenuates Doxorubicin-induced podocyte foot process effacement [17]. Also, According to FIELD study, DAIS study, and ACCORD Lipid study, fenofibrate was proved to reduce microalbuminuria in diabetic patients [18, 19, 20, 21]. Thus we speculated that fenofibrate might contribute to differentiate podocytes. In this manuscript we treated E11 podocytes with 200μM of fenofibrate suspended in dimethyl sulfoxide.

Transfection of E11 podocytes

E11 podocytes were suspended by mild trypsinization and electroporated with CsCl double banding plasmid under low-voltage condition (0.2kV, 950μF) [16]. The cells were then allowed to adhere to culture dishes for 30-48 h. Twelve hours following electroporation, either dimethyl sulfoxide (1:1,000 dilution) or 200μM of fenofibrate was added to the fresh culture medium to induce E11 podocyte cell differentiation.

Immunoprecipitation and Immunoblotting

Scraped frozen cells were rocked for 10 min at 4°C with NP-40 lysis buffer (25mM Hepes, pH 7.4, 10% glycerol, 1% NP-40, 50mM sodium fluoride, 10mM sodium phosphate, 137mM sodium chloride, 1mM sodium orthovanadate, 1mM PMSF, 10μg/mL aprotinin, 1μg/mL pepstatin, 5μg/mL leupeptin). Insoluble material was separated from the soluble extract by centrifugation for 10 min at 4°C, and the total protein amount in the supernatant was determined by BCA method. Immunoprecipitations were performed by using 2mg of the cell extracts incubated with 4 μg of a Septin7 polyclonal antibody for 2 hours at 4°C. The samples were then incubated with protein A-Sepharose for 1 hour at 4°C. Either immunoprcipitaed samples or whole cell lysates samples were resuspended in SDS sample buffer (125mM Tris-HCl, pH 6.8, 20% (v/v) glycerol, 4% (w/v) SDS, 100mM dithiothreitol, 0.1%

(w/v) bromophenol blue), and heated at 100 ^{0}C for 5 min. Samples were separated by SDS polyacrylamide gel electrophoresis (SDS-PAGE) and electrophoretically transferred to polyvinylidene difluoride membranes. The samples were immunoblotted with monoclonal or polyclonal specific antibody.

GST fusion protein precipitation

Cell lysates from E11 podocytes treated with 200μM of fenofibrate were incubated with either GST alone or with GST-Nucleobindin-2 fusion proteins immobilized on glutathione-agarose beads for 1 hour at 4°C [22]. The beads were extensively washed three times with the lysis buffer. The retained proteins were eluted with SDS-sample buffer, heated at 100°C for 5 min and separated by SDS-PAGE. The gel was stained by GelCode Blue Stain Reagent (PIERCE) following the manufacture's instruction.

TOF-Mass analysis

TOF-Mass analysis was submitted to Filgen, Inc. (Nagoya, Japan).

Quantification of insulin-stimulated GLUT4 translocation

Quantification of transfected GLUT4 translocation was determined using a qualitative colorimetric assay as previously described [16, 23]. Briefly, E11 podocytes were co-transfected with 200μg of eGFP-cMyc-GLUT4 plus 400μg of various other cDNAs as indicated in each figure. Following basal or hormonal stimulation, the cells were cooled to 4°C and incubated with a myc antibody followed by an HRP-conjugated anti-myc antibody. The specific cell surface bound HRP was then determined by incubation with the o-phenylenediamine dihydrochloride peroxidase substrate.

Statistical analysis

All values are expressed as mean +/- standard deviation (S.D.). Data were evaluated for statistical significance by analysis of variance and *t* test using the InStat 2 program.

Results

Effect of fenofibrate on E11 podocytes

The FIELD, DIAS and ACCORD Lipid studies indicated that fenofibrate was effective at reducing microalbuminuria in diabetic patients [18, 19, 20, 21]. Fenofibrate is a selective peroxisome proliferator-activated receptor-α (PPARα) agonist that is renal-protective and attenuates doxorubicin-induced podocytes foot process effacement [17]. However there are no reports studyting whether PPARα agonist affects podocytes differentiation. To explore this possibility, we treated E11 cells with and without fenofibrate. E11 podocytes treated with 200μM of fenofibrate resulted in a dramatic morphological change after 8 hours and were substantially elongated with increased arborization by 24 hours. In contrast, the E11 cells in the absence of fenofibare did not undergo any significant morphological change (Fig. 1A b, c).

In Fig. 1B, we confirmed that fenofibrate treated E11 podocytes expresses podocytes specific markers as GPR137B, Clic5, Nephrin, and GLUT4 by western blotting (Fig. 1B). Having established transient transfection [9-16] and modified differentiation strategy, we estimated GLUT4 translocation of cultured podocytes with or without fenofibrate treatment using a GLUT4 reporter construct. As shown in Fig. 1C-a, insulin was an ineffective stimulator of GLUT4 translocation in undifferentiated E11 cells. In contrast, following fenofibrate treatment, insulin was capable of inducing an approximately 2-fold stimulation of GLUT4 translocation (Fig. 1C-b). This extent of insulin-stimulated GLUT4 translocation is similar to that previously reported using a conventional culture and differentiation protocol [12, 14, 16].

Nucleobindin-2 was identified as a binding partner for Septin7

To screen for potential Nucleobindin-2 binding partners in podocytes, we mixed either GST or GST-Nucleobindin-2 with lysates from differentiated E11 podocytes followed by SDS-PAGE and the gel was stained with GelCode Blue (Fig. 2A). The approximately 50 kDa band indicated by the arrow in the GST-Nucleobindin-2 lane was cut out and applied to TOF mass spectrometry analysis for sequence identification and multiple peptide sequences for Septin7 were found. Immunoprecipitaion of Septin7 from control and insulin-stimulated cells demonstrated that Septin7 directly binds to Nucleobindin-2, consistent with the mass spectroscopy identification. However, there was no significant effect of insulin on the Septin7/Nucleobindin-2 interaction (Fig. 2B). Having a high quality of transfection efficacy [16], we introduced Nucleobindin-2 RNAi that reduced Nucleobindin-2 protein levels by

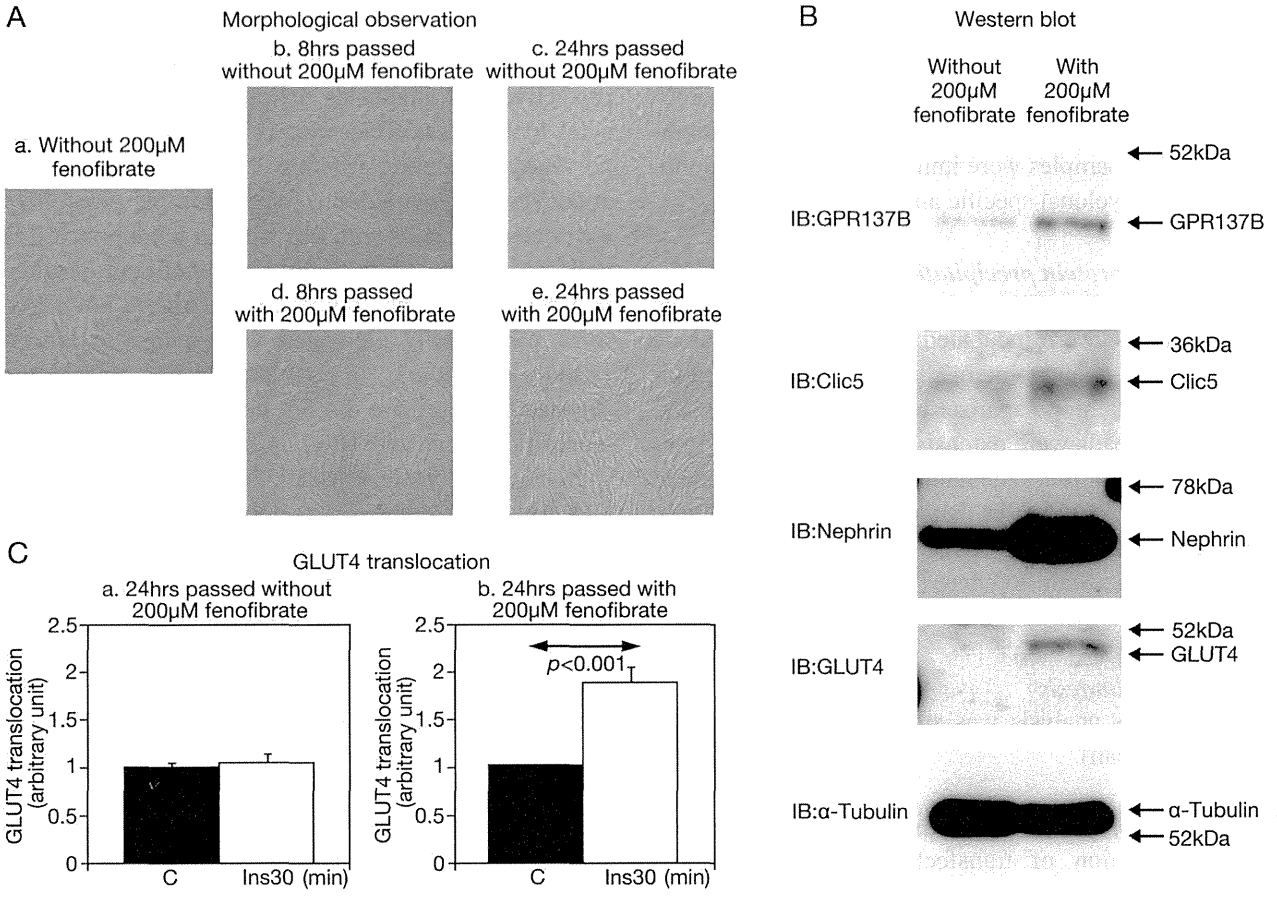

Fig. 1 Effect of fenofibrate on E11 podocytes

A) 200μM of fenofibrate started show morphological change 8 hours later (Fig. 1A-d) and completely changed E11 podocytes as shown Fig. 1A-e. As a control, vehicle alone did not make any change (Fig. 1A-b, 1A-c). Data show representative experiments independently performed and each experiment was repeated three times.

B) Estimation of quality about fenofibrate treated E11 podocytes is shown by western blotting. In this panel podocytes specific marker proteins such as GPR137B, Clic5, and Nephrin are compared between fenofibrate untreated (left lane) and treated (right lane) E11 cells. α-Tubulin blotting tells us each lane has equal protein loading amount. Data show representative experiments independently performed and each experiment was repeated three times.

C) Estimation of GLUT4 translocation of E11 podocytes without or with fenofibrate treatment is represented. On the left panel (Fig. 1C-a), GLUT4 translocation evaluated by colorimetric assay in E11 podocytes without fenofibrate is shown and on the right panel (Fig. 1C-b) GLUT4 translocation evaluated by colorimetric assay in E11 podocytes with fenofobrate is shown. Experiments were independently performed three times and expressed as the mean ± S.D.

approximately 60-70% (Fig. 2C, upper panel). The reduction in Nucleobindin-2 protein had no significant effect on Septin7 protein levels (Fig. 2C, lower panel). However, the loss of Nucleobindin-2 resulted in a near complete inhibition of insulin-stimulated GLUT4 translocation with no significant effect on the basal level of cell surface GLUT4 protein (Fig. 2D). Theses data suggested that endogenous Nucleobindin-2 is required for insulin-stimulated GLUT4 translocation and may function as an inhibitor Septin7.

Discussion

Recently Nucleobindin-2 was reported to regulate insulin secretion, peripheral glucose uptake, and hepatic gluconeogenesis and decreased Nucleobindin-2 expression has been suggested to partly account for several metabolic consequences in diabetic animal models [8-11]. In addition to the regulation of insulin secretion and sensitivity in peripheral tissues, Nucleobindin-2/Nesfatin-1 proteins have also been shown to regulate hypothalamic function in the control of hepatic glu-

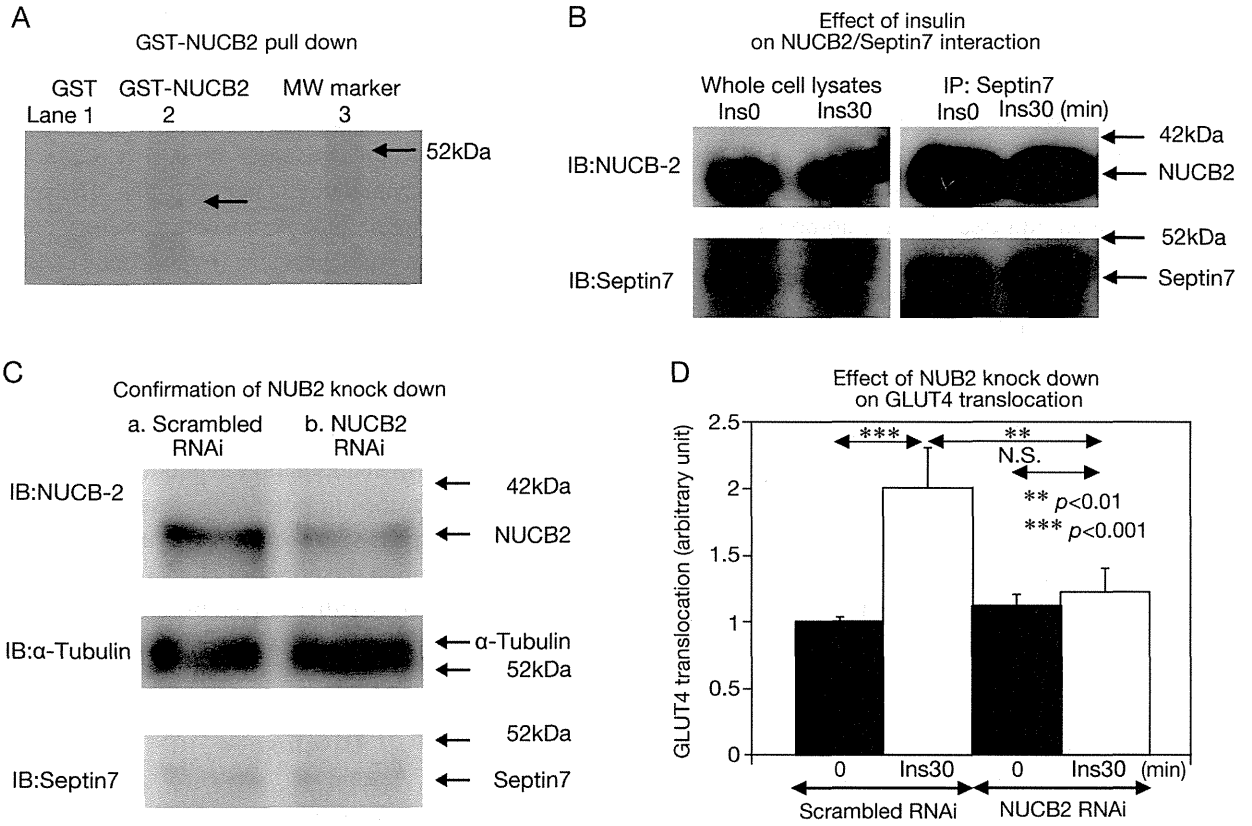

Fig. 2 Nucleobindin-2 was identified as a binding partner for Septin7

A) We mixed either GST (lane 1) or GST-Nucleobindin-2 (lane 2) with clear lysates from E11 podocytes with fenofibrate treatment and run on SDS-PAGE. The gel was conducted to GelCode Blue staining and the specific band (indicated by arrow in lane 2) for GST-Nucleobindin-2 around 50 kDa was cut out and applied to TOF Mass analysis to identify the molecules. Data show representative experiments independently performed and each experiment was repeated three times.

B) Co-immunoprecipitation experiment results by using Septin7 specific antibody is shown in lower panel. The samples were obtained from cells treated without or with 100nM insulin stimulation for 30 min. In the upper panel, Nucleobindin-2 (NUCB2) amount associated Septin 7 is shown. Theses experiments were independently performed three times.

C) We introduced Nucleobindin-2 RNAi by electroporation to knock down Nucleobindin-2 and reduced Nucleobindin-2 expression by 60-70% compared to control samples transfected with scrambled RNAi. Data show representative experiments independently performed and each experiment was repeated four times.

D) Estimation of Nucleobondin-2 knock down effect on insulin-stimulated GLUT4 translocation in E11 podocytes is shown. GLUT4 translocation was estimated by colorimetric assay in the presence of 200μM of fenofibrate in E11 podocytes. Theses experiments were independently performed three times and expressed as the mean ± S.D.

cose production [10]. Despite these studies, the functional role if any for Nucleobindin-2 in kidney function particularly podocytes insulin action has not been addressed.

Fenofibrate was reported to protect podocytes from doxorubicin-induced injury [17] but until today there are no reports to clearly state that fenofibrate alone can differentiate podocytes. We demonstrated that fenofibrate treated E11 podocytes showed morphological change resembling those reported for the differentiation of E11 podocytes by the conventional method [12, 14]. In addition, we observed the up regulation of several podocyte specific markers (GPR137B, Clic5, and Nephrin) indicating the formation of a podocyte phenotype [24]. It is important to note that the fenofibrate treatment required only 2 days of treatment and was as effective to the previous reported method that requires 7-10 days. In any case, our results are consistent with a previous large-scale clinical trial showing that fenofibrate administration protects against microalbuminuria in diabetic patients [18-21]. As PPARγ was also reported to have renal protective function [14], future

studies are needed to examine the relative contributions of PPARα and/or PPARγ agonist in the differentiation response.

In this report we also described a colorometric assay for the quantification of GLUT4 translocation in differentiated podocytes that was originally developed for differentiated cultured 3T3-L1 adipocytes. In this assay we need to express an exofacial myc tagged GLUT4 and to perform the assay within 48 hours after the transfection as differentiated podocytes due to the transient nature of myc-GLUT4 expression. The ability of fenofibrate to induce E11 podocyte cell differentiation within this time frame is necessary for the successfulness of this approach.

This report presents evidence that Nucleobindin-2 is expressed in podocytes and that Nucleobindin-2 is a Septin7 binding partner, although this interaction does not appear to be regulated by insulin. In several cell types the cellular localization of Nucleobindins appears to be variable with a distributions reported in most subcellular compartments [1-7] and the subcellular distribution within podocytes remains to be examined. A previous study indicated that Septin7 inhibits insulin-stimulated glucose uptake by blocking Nephrin-VAMP2 interactions [13]. Therefore Nucleobindin-2 expression status is potentially one mechanism to depress this inhibition. Interestingly, recently a podocyte specific GLUT4 knockout mouse phenotype (podocytes specific insulin resistance model) was reported to be protective from diabetic nephropathy. The report suggested that there might exist a compensatory mechanism to increase podocytes size (hypertrophy) despite a reduction in podocytes number [25]. In human being it is less likely to happen that GLUT4 null situation in podocytes but there might exist similar compensation mechanism exists and if so if it is impaired in diabetic patients, treatment of insulin resistance from the point of Nucleobindin-2 manipulation in podocytes would be a promising approach to potentially rescue the risk of diabetic nephropathy. In addition, future studies are needed to determine the effect of Nucleobindin-2 deficiency *in vivo* and whether Nucleobindin-2 expression is altered under various physiologic and pathophysiologic states.

Disclosure

All the authors declared no competing interests.

References

1. Gonzales R, Mohan H, Unniappan S (2012) Nucleobindins: Bioactive precursor proteins encoding putative endocrine factor? *Gen Comp Endocrinol* 176: 341-346.
2. Wang S, Miyauchi M, Koshikawa N, Maruyama K, Kubota T, *et al.* (1994) Antigen expression associated with lymph node metastasis in gastric adenocarcinomas. *Pathol Int* 44: 844-849.
3. Miura K, Titani K, Kurosawa Y, Kanai Y (1992) Molecular cloning of nucleobindin, a novel DNA-binding protein that contains both a signal pep- tide and a leucine zipper structure. *Biochem Biophys Res Commun* 187: 375-380.
4. Wendel M, Sommarin Y, Bergman T, Heinegard D (1995) Isolation, characterization, and primary structure of a calcium-binding 63-kDa bone protein. *J Biol Chem* 270: 6125-6133.
5. Ballif BA, Mincek NV, Barratt JT, Wilson ML, Simmons DL (1996) Interaction of cyclooxygenases with an apoptosis- and autoimmunity-associated protein. *Proc Natl Acad Sci USA* 93: 5544-5549.
6. Lin P, Le-Niculescu H, Hofmeister R, McCaffery JM, Jin M, *et al.* (1998) The Mammalian Calcium-binding Protein, Nucleobindin (CALNUC), Is a Golgi Resident Protein. *J Cell Biol* 141: 1515-1527.
7. Karabinos A, Bhattacharya D, Kratzin HD, Hilschmann N (1998) Origin of the NEFA and Nuc signal sequences. *J Mol Evol* 46: 327-333.
8. Oh-I S, Shimizu H, Satoh T, Okada S, Adachi S, *et al.* (2006) Identification of nesfatin-1 as a satiety molecule in the hypothalamus. *Nature* 443: 709-712.
9. Foo KS, Brauner H, Ostenson CG, Broberger C (2010) Nucleobindin-2/nesfatin in the endocrine pancreas: distribution and relationship to glycaemic state. *J Endocrinol* 204: 255-263.
10. Wu D, Yang M, Chen Y, Jia Y, Ma ZA, *et al.* (2014) Hypothalamic Nesfatin-1/NUCB2 Knockdown Augments Hepatic Gluconeogenesis that is Correlated with Inhibition of mTOR-STAT3 Signaling Pathway in Rats. *Diabetes* 63: 1234-1247.
11. Feijóo-Bandín S, Rodríguez-Penas D, García-Rúa V, Mosquera-Leal A, Otero MF, *et al.* (2013) Nesfatin-1 in human and murine cardiomyocytes: synthesis, secretion, and mobilization of GLUT-4. *Endocrinology* 154: 4757-4767.
12. Wasik AA, Polianskyte-Prause Z, Dong MQ, Shaw AS, Yates JR 3rd, *et al.* (2012) Septin 7 forms a complex with CD2AP and nephrin and regulates glucose trans-

porter trafficking. *Mol Biol Cell* 23: 3370-3379.
13. Lay A, Coward RJ (2014) Recent advances in our understanding of insulin signaling to the podocyte. *Nephrol Dial Transplant* 29: 1127-1133.
14. Kanjanabuch T, Ma LJ, Chen J, Pozzi A, Guan Y, Mundel P, *et al.* (2007) PPAR-γ agonist protects podocytes from injury. *Kidney Int* 71: 1232-1239.
15. Okada S, Mori M, Pessin JE (2003) Introduction of DNA into 3T3-L1 adipocytes by electroporation. *Methods Mol Med* 83: 93-96.
16. Yamada E, Saito T, Okada S, Takahashi H, Ohshima K, *et al.* (2014) Synip phosphorylatuion is required for insulin-stimulated Glut4 translocation and glucose uptake in podocyte. *Endocr J* 61: 523-527.
17. Zhou Y, Kong X, Zhao P, Yang H, Chen L, *et al.* (2011) Peroxisome proliferator-activated receptor-α is renoprotective in doxorubicin-induced glomerular injury. *Kidney Int* 79: 1302-1311.
18. Keech AC, Grieve SM, Patel A, Griffiths K, Skilton M, *et al.* (2005) Urinary albumin levels in the normal range determine arterial wall thickness in adults with Type 2 diabetes: a FIELD substudy. *Diabet Med* 22: 1558-1565.
19. Ansquer JC, Foucher C, Rattier S, Taskinen MR, Steiner G, *et al.* (2005) Fenofibrate reduces progression to microalbuminuria over 3 years in a placebo-controlled study in type 2 diabetes: results from the diabetes atherosclerosis intervention study (DAIS). *Am J Kidney Dis* 45: 485-493.
20. Mychaleckyj JC, Craven T, Buse J, Crouse JR, Elam M, *et al.* (2012) Reversibility of fenofibrate therapy–induced renal function impairment in ACCORD type 2 diabetic participants. *Diabetes Care* 35: 1008-1014.
21. Simo R, Roy S, Behar-Cohen F, Keech A, Mitchell P, *et al.* (2013) Fenofibrate: a new treatment for diabetic retinopathy. Molecular mechanisms and future perspectives. *Curr Med Chem* 20: 3258-3266.
22. Holt KH, Waters SB, Okada S, Yamauchi K, Decker SJ, *et al.* (1996) Epidermal growth factor receptor targeting prevents uncoupling of the Grb2-SOS complex. *J Biol Chem* 271: 8300-8306.
23. Yamada E, Okada S, Saito T, Ohshima K, Sato M, *et al.* (2005) Akt2 phosphorylates Synip to regulate docking and fusion of GLUT4-containing vesicles. *J Cell Biol* 168: 921-928.
24. Pierchala BA, Muñoz MR, Tsui CC (2010) Proteomic analysis of the slit diaphragm complex: CLIC5 is a protein critical for podocyte morphology and function. *Kidney Int* 78: 868-882.
25. Guzman J, Jauregui AN, Merscher-Gomez S, Maiguel D, Muresan C, *et al.* (2014) Podocyte-specific GLUT4-deficient mice have fewer and larger podocytes and are protected from diabetic nephropathy. *Diabetes* 63: 701-714.

Endocrine Journal 2014, **61** (8), 825-832

RAPID COMMUNICATION

Somatic mutations of the catalytic subunit of cyclic AMP-dependent protein kinase (*PRKACA*) gene in Japanese patients with several adrenal adenomas secreting cortisol

Yasuyo Nakajima[1)*], Takashi Okamura[1)*], Tamae Gohko[1)], Tetsurou Satoh[1)], Koshi Hashimoto[1)], Nobuyuki Shibusawa[1)], Atsushi Ozawa[1)], Sumiyasu Ishii[1)], Takuya Tomaru[1)], Kazuhiko Horiguchi[1)], Shuichi Okada[1)], Daisuke Takata[2)], Nana Rokutanda[2)], Jun Horiguchi[2)], Yoshito Tsushima[3)], Tetsunari Oyama[4)], Izumi Takeyoshi[2)] and Masanobu Yamada[1)]

[1)] *Department of Medicine and Molecular Science, Gunma University Graduate School of Medicine, Maebashi 371-8511, Japan*
[2)] *Department of Thoracic and Visceral Organ Surgery, Gunma University Graduate School of Medicine, Maebashi 371-8511, Japan*
[3)] *Department of Diagnostic Radiology and Nuclear Medicine, Gunma University Graduate School of Medicine, Maebashi 371-8511, Japan*
[4)] *Department of Diagnostic Pathology, Gunma University Graduate School of Medicine, Maebashi 371-8511, Japan*

Abstract. Somatic mutations of the catalytic subunit of the cyclic AMP-dependent protein kinase (*PRKACA*) gene have recently been identified in about 35% of cortisol-producing adenomas (CPAs), with the affected patients showing overt Cushing's syndrome. Since we recently reported higher prevalence of mutations of the *KCNJ5* gene and associations with autonomous cortisol secretion in Japanese aldosterone-producing adenomas than in Western countries, there might be different features of CPAs between Japan and the West. We therefore investigated mutations of the *PRKACA* gene in Japanese patients with several adrenal tumors secreting cortisol, including overt Cushing's syndrome, subclinical Cushing's syndrome, and aldosterone-producing adenomas (APAs) co-secreting cortisol operated on at Gunma University Hospital. Of the 13 patients with CPA who showed overt Cushing's syndrome, 3 (23%) had recurrent somatic mutations of the *PRKACA* gene, p.L206R (c.617 T>G), and there were no mutations in subclinical Cushing's syndrome. Among 33 APAs, 24 had somatic mutations of the *KCNJ5* gene, either G151R or L168R, 11 (33%) had autonomous cortisol secretion, but there were no mutations of the *PRKACA* gene. We established a PCR-restriction fragment length polymorphism assay and revealed that the mutated allele was expressed at a similar level to the wild-type allele. These findings demonstrated that 1) the prevalence of Japanese patients with CPA who showed overt Cushing's syndrome and whose somatic mutations in the *PRKACA* gene was similar to that in Western countries, 2) the mutation might be specific for CPAs causing overt Cushing's syndrome, and 3) the mutant *PRKACA* allele was expressed appropriately in CPAs.

Key words: *PRKACA*, Cortisol-producing adenomas, Japanese

OVERPRODUCTION of adrenal cortisol induces several characteristic manifestations, including moon face, buffalo hump, striae, thin skin, and central obesity, known as Cushing's syndrome [1, 2]. Tumors secreting cortisol in patients who did not show any symptoms typical of Cushing's syndrome were described as subclinical Cushing's syndrome [1, 3, 4], but this concept is not universal, and the definition differs among investigators and countries [5, 6]. In addition, we and others, particularly Japanese investigators, have reported an association of primary aldosteronism with mild autonomous cortisol secretion [7-9].

The mechanisms underlying the tumorigenesis of adrenal cortisol-producing adenomas (CPAs) and autonomous cortisol production are still largely unknown. However, Beuschlein *et al.* recently successfully identified the recurrent somatic mutation p.L206R (c.617T>G) by exome analysis in the gene encoding *PRKACA*, which encodes the catalytic sub-

Submitted Jun. 13, 2014; Accepted Jun. 19, 2014 as EJ14-0282
Released online in J-STAGE as advance publication Jul. 25, 2014

Correspondence to: Masanobu Yamada, M.D., Ph.D., Department of Medicine and Molecular Science, Gunma University Graduate School of Medicine, 3-39-15 Showa-machi, Maebashi, Gunma 371-8511, Japan. E-mail: myamada@gunma-u.ac.jp
*These two authors contributed equally to this work.

unit of cyclic AMP-dependent protein kinase (protein kinase A [PKA]), in 22 of 59 (37%) patients with CPA who showed overt Cushing's syndrome [10].

Goh *et al.* also identified the *PRKACA* mutation encoding p.L206R at a similar prevalence, namely, 35% of PCAs associated with overt Cushing's syndrome [11]. Leu206 directly interacts with the regulatory subunit of PKA, PRKAR1A. The hotspot p.L206R mutation causes loss of this PRKAR1A binding, increasing the phosphorylation of downstream targets and causing constitutive activation of the PKA catalytic subunit, which induces overproduction of cortisol and cell proliferation [11].

We have recently reported high prevalence of somatic mutation in a potassium channel gene, *KCNJ5*, of approximately 70%, in Japanese patients with adrenal aldosterone-producing adenomas (APAs) and some APAs co-secreting cortisol [12, 13]. In contrast, in Western countries, the prevalence of the mutations has been reported to be approximately 35-40% of APAs, and cases of APAs co-secreting cortisol have rarely been reported [14].

Therefore, there may be differences of *PRKACA* mutations in CPAs and adrenal cortisol-secreting adenomas between Japan and Western countries. In the present study, we investigated the *PRKACA* mutations in several adrenal tumors secreting cortisol, including overt Cushing's syndrome, subclinical Cushing's syndrome, and APAs co-secreting cortisol.

Subjects and Methods

Subjects

We reviewed the medical records of 21 patients with CPA and 33 patients with APA, who were operated on at Gunma University Hospital during the period 2007-2013. Each subject provided written informed consent, and the study was approved by the ethics committee on human research of Gunma University. The diagnosis of Cushing's syndrome was made in 13 female cases (aged 54 ± 13 yr (mean ± SD)) according to guidelines published by the Endocrine Society [1]. The diagnosis of primary aldosteronism (PA) was initially performed as previously reported [7, 15]. We also examined morning and midnight cortisol levels, as well as 1 mg dexamethasone suppression test (DST) results in all the patients with suspected PA [7, 8, 16]. Failure of cortisol to suppress the level to less than 3.0 μg/dl (139.75 nmol/L) in the DST was used as a parameter for autonomous cortisol secretion in this study.

Plasma aldosterone levels were measured with the RIA SPAC-S Aldosterone kit TFB; plasma renin activity, with the RIA Renin IRMA KIT "Daiichi" TFB; plasma cortisol, with the RIA Cortisol kit "TFB" TFB; and ACTH, with ECLIA Eclusys ACTH by Roche Diagnostics.

RNA extraction and detection of mutations of PRKACA cDNA by PCR and direct sequencing

All specimens of adrenal tumor were frozen in liquid nitrogen immediately after removal during operation. Total RNA was prepared from each adenoma using ISOGEN (Nippongene, Toyama, Japan) according to manufacturer's instructions. Then, cDNA was reverse-transcribed from 300 ng of total RNA (TaqMan Reverse Transcription Reagents, Applied Biosystems, Tokyo, Japan). To sequence the *PRKACA* cDNA, 1.0 μL of cDNA was used for the polymerase chain reaction (PCR), as previously reported [17]. PCR solutions were prepared according to the manual for AmpliTaq (Life Technologies, Carlsbad, CA, USA) with a final volume of 50 μL. Each primer used for PCR was set in a different exon, 5'F1, 5'-CCTGACCTTTGAGTATCTGCACT-3' (forward primer) and h3'R1, 5'-CGGCCATTTCATAGATAAGA ACC-3' (reverse primer) in putative exons 6 and 7 (ENST00000308677). After denaturing for 2 min at 94°C, amplification was performed for 35 cycles at 94°C for 30 sec, 58°C for 30 sec, and 72°C for 1 min using a GeneAmp PCR system 9700 (Applied Biosystems, Tokyo, Japan). The PCR products (244 bp) were purified with an AxyPrep PCR clean-up kit (AXYGEN Biosciences, Union City, CA, USA) for sequencing. These samples were directly sequenced using an Applied Biosystems 3730xl (Applied Biosystems, Tokyo, Japan).

In cases in which mutation of the *PRKACA* gene was identified, we sequenced the mutated nucleotide of the genomic DNA from peripheral blood using primers 5'-GTTTCTGACG GCTGGACTG-3' and 5'-CGGCCATTTCATAGATAAGAACC-3' under the same PCR conditions as described above.

PCR-RFLP assay

We performed a polymerase chain reaction-restriction fragment length polymorphism assay (PCR-RFLP) in CPAs with p.L206R (c.617T>G), since this mutation produces a site that cannot be digested with the BciT130 I (EcoR II, Mva I) (Takara Shiga, Japan)

restriction enzyme. The 213-bp fragment encompassing the 617T>G mutation in cDNA was generated using the primers 5'-CCTGACCTTTGAGTATCTGCACT-3' and 5'-CACCAGTCCACGGCCTTGTTGTA-3'. PCRs were performed as above. The wild-type cDNA was cut with BciT130 I into two fragments of 162 bp and 52 bp (not detected), while the mutated allele remained uncut, and similarly the wild-type genomic DNA was cut into fragments 127 bp and 147 bp in length. The fragments were resolved on a 2% agarose gel. We compared the density of the 213-bp and 162-bp fragments after digestion to evaluate the ratio of levels of the mutated and wild-type *PRKACA* mRNA. The bands were quantitatively measured using Molecular Imager FX (Bio-Rad Laboratories, Inc., Tokyo, Japan). All experiments were repeated at least twice.

Statistical analysis

All results are expressed as the mean ± SD for continuous variables and as absolute numbers. Statistical analyses were performed with ANOVA and Student's *t* test using JMP 10.0.2 (SAS Institute Inc., Cary, NC).

Results

Mutations of the PRKACA gene in patients with CPAs and other adrenal adenomas secreting cortisol

Table 1 shows the clinical features of patients with Cushing's syndrome. All patients showed symptoms typical of Cushing's syndrome. Mean tumor size (maximum diameter) on CT was 28 ± 4 mm. The 24-h urinary free cortisol excretion in 12 patients was over 200 μg/day, except for 1 case with 81.8 μg/day. In all patients, plasma ACTH levels were undetectable (Table 1). Furthermore, the pathology in all cases was confirmed as adrenocortical adenoma. We examined mutation of the *PRKACA* gene in these 13 patients and found that 3 CPAs had somatic mutations of the *PRKACA* gene. As shown in Fig. 1 (lower panel), mutations were concentrated at nucleotide T 617 bp downstream of the translation start site, and the conversion of T to G causing the substitution of leucine (L) by arginine (R) at residue 206 (p.L206R), which is the same substitution as reported by Beuschlein *et al.* [10]. Furthermore, we also confirmed that there were no germline mutations of *PRKACA* in DNA from

Table 1 Clinical features of 13 patients with Cushing's syndrome

Pt	Age (yr)	Sex	Specific cushingoid signs (Yes/No)	Metabolic disorders (Yes/No)				complications	ACTH (pg/mL)	Midnight serum cortisol (μg/dL)	24 h urine cortisol (μg/day)	1 mg DST (μg/dL)	Tumor Size (mm)	*PRKACA* mutation
				obesity	HT	HL	DM/IGT							
1	37	F	Yes	Yes	Yes	Yes	Yes	renal stone	1.0	13.8	295	15.4	28	c.617 T>G (p.L206R)
2	67	F	Yes	Yes	Yes	Yes	Yes		<5	25.4	249	33.0*	20	c.617 T>G (p.L206R)
3	68	F	Yes	No	Yes	Yes	Yes	osteoporosis, primary aldosteronism***	1.0	13.3	81.8	12.8	21	c.617 T>G (p.L206R)
4	71	F	Yes	Yes	Yes	Yes	Yes		<5	22.4	405	39.9	30	Wild type
5	63	F	Yes	Yes	Yes	Yes	Yes	hyperparathyroidism	1.0	17.0	446	27.2	26	Wild type
6	59	F	Yes	Yes	Yes	Yes	Yes		1.0	15.8	331	**	25	Wild type
7	54	F	Yes	Yes	Yes	Yes	Yes	stroke	<5	17.2	492	16.9	30	Wild type
8	33	F	Yes	Yes	Yes	Yes	Yes		<5	20.0	477	19.9	32	Wild type
9	41	F	Yes	Yes	Yes	No	No	small intestine tumor	1.0	13.7	205	15.7	36	Wild type
10	44	F	Yes	No	Yes	No	No	fracture, stroke, renal stone	1.0	13.4	318	13.9	30	Wild type
11	65	F	Yes	Yes	Yes	Yes	Yes	fracture	1.0	23.1	217	27.9*	26	Wild type
12	52	F	Yes	Yes	Yes	No	Yes	uterine fibroids	1.0	15.6	267	16.8	27	Wild type
13	42	F	Yes	Yes	Yes	Yes	Yes	osteoporosis, gastric ulcer	1.0	21.7	272	24.2	30	Wild type

PRKACA mutation represents a heterozygous mutation of c.617 T>G (p.L206R). M, male; F, female. Specific cushingoid signs refer to the guidelines of the Endocrine Society. HT, hypertension,The diagnosis of hypertension was made according to the 2014 guidelines of The Japanese Society of Hypertension. DM/IGT includes diabetes mellitus and impaired glucose tolerance, The diagnosis of diabetes mellitus and glucose tolerance were made according to the 2006-2007 guidelines of The Japan Diabetes Society. HL, hyperlipidemia, Hyperlipidemia was evaluated according to the 2007 guidelines of Japan Atherosclerosis Society. 1 mg DST, serum cortisol levels in the 1 mg dexamethasone suppression test. Tumor size is the maximum diameter of the tumor observed in the CT study. *Pt. 2 and Pt. 11 underwent 8 mg dexamethasone suppression test. **No data were available. ***Pt. 3 was diagnosed with primary aldosteronism at the opposite side of cortisol-producing adenoma by performing adrenal vein sampling.

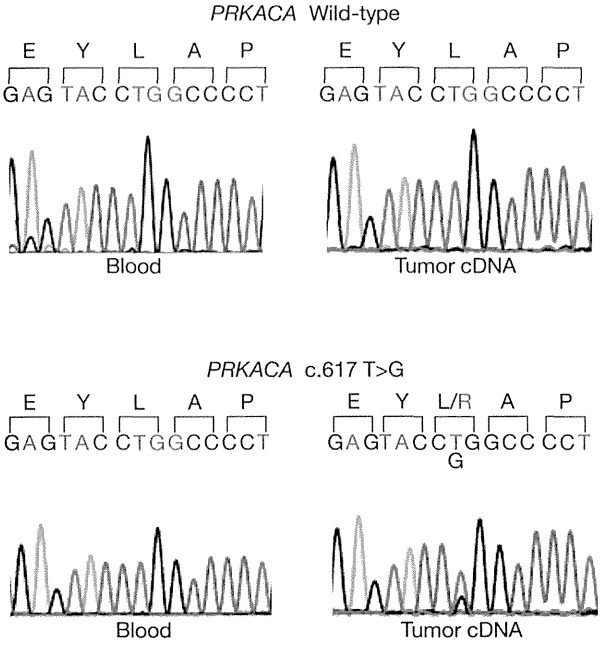

Fig. 1 Sequences of mutations of the *PRKACA* gene in CPAs
Representative sequences of peripheral blood DNA (Blood) and tumor cDNA of the mutant *PRKACA* are depicted. L206R T/G represents heterozygosity for an T-to-G transition 617 bp from the translation start site in the *PRKACA* gene, resulting in a leucine-to-arginine substitution at codon 206 (c.617T>G, p.L206R). No mutations were identified in the peripheral blood DNA.

peripheral blood of the 3 patients with mutations (lower panel, Blood).

As shown in Table 2, we next examined the tumors of 8 patients who showed autonomous cortisol secretion. Serum ACTH levels in most patients were below 10 pg/mL, except for patient 2 with 14.9 pg/mL. Fractionated urine cortisol levels were within normal limits or slightly elevated, but below 150 μg/day. None of the patients showed suppression of serum cortisol level below 3 μg/dL after overnight loading of 1 mg of dexamethasone (1 mg DST). Mean tumor size was 32 ± 10 mm. We found no mutations of the *PRKACA* gene in these 8 adenomas.

Table 3 shows the clinical features of 33 cases of APAs. Among these APAs, 24 were harboring somatic *KCNJ5* mutations of either G151R or L168R, and 11 had autonomous cortisol secretion. None of the patients had any Cushingoid signs, except patient 11 in Table 3, who showed a slight moon face. However, these 11 cases showed no suppression of serum cortisol level below 3 μg/dL by 1 mg DST. As seen in tumors showing subclinical Cushing's syndrome, urine cortisol levels of these 11 patients were within the normal range or slightly high, but below 150 μg/day. We examined the mutation of the *PRKACA* gene in all of the 33 APAs, but there were no such mutations in tumors showing

Table 2 Clinical features of 8 patients with subclinical Cushing's syndrome

Pt	Age (yr)	Sex	Specific cushingoid signs (Yes/No)	Metabolic disorders (Yes/No)				complications	ACTH (pg/mL)	Midnight serum cortisol (μg/dL)	24 h urine cortisol (μg/day)	1 mg DST (μg/dL)	Tumor Size (mm)	*PRKACA* mutation
				obesity	HT	HL	DM/IGT							
1	57	F	No	Yes	Yes	Yes	Yes		8.8	5.0	25.2	3.4	35	Wild type
2	54	F	No	Yes	Yes	Yes	Yes	breast cancer	14.9	3.9	16.1	4.0	15	Wild type
3	69	F	No	Yes	Yes	Yes	Yes	primary aldosteronism*** Grave's disease	1.0	9.4	51	12.4*	30	Wild type
4	48	F	No	No	No	No	No		6	**	133	16.3	35	Wild type
5	76	F	No	No	Yes	No	No	stroke	<5	**	43.6	6.8	30	Wild type
6	66	M	No	No	Yes	No	No		7.9	8.0	94.6	5.5	22	Wild type
7	73	F	No	No	Yes	No	No		6.7	4.0	29.1	3.8	40	Wild type
8	60	F	No	Yes	Yes	Yes	Yes	arteriosclerosis obliterans	5.0	9.6	71.4	12.9	48	Wild type

PRKACA mutation represents a heterozygous mutation of c.617T>G (p.L206R). M, male; F, female. Specific cushingoid signs refer to the guidelines of the Endocrine Society. HT, hypertension. DM/IGT includes diabetes mellitus and impaired glucose tolerance. HL, hyperlipidemia. 1 mg DST, serum cortisol levels in the 1 mg dexamethasone suppression test. Tumor size is the maximum diameter of the tumor observed in the CT study. *Pt. 3 underwent 8 mg dexamethasone suppression test. **No data were available. ***Pt. 3 was diagnosed with primary aldosteronism at the opposite side of cortisol-producing adenoma by performing adrenal vein sampling.

Table 3 Clinical features of 33 patients with aldosterone-producing adenoma with or without hypercortisolism

Pt	Age (yr)	Sex	Specific cushingoid signs (Yes/No)	Mild hypercortisolism (Yes/No)	PAC (pg/mL)	PRA (ng/mL/h)	1 mg DST	ACTH (pg/mL)	Midnight serum cortisol (μg/dL)	24 h urine cortisol (μg/day)	*PRKACA* mutation (Yes/No)	*KCNJ5* Mutation
1	30	F	No	Yes	580	0.3	Yes	16.4	6	37.1	No	c.451G>A (p.G151R)
2	53	F	No	Yes	393	0.1	Yes	34	11.4	118	No	c.503T>G (p.L168R)
3	48	F	No	Yes	888	0.4	Yes	16.7	3.4	44	No	c.503T>G (p.L168R)
4	60	F	No	Yes	114	0.4	Yes	<5	10.5	86.5	No	Wild type
5	48	F	No	Yes	231	0.4	Yes	6.8	5	35.9	No	Wild type
6	57	M	No	Yes	526	0.1	Yes	31.6	5.1	32.8	No	c.451G>A (p.G151R)
7	58	M	No	Yes	742	<0.1	Yes	14	5.4	59.1	No	c.451G>C (p.G151R)
8	75	M	No	Yes	132	0.2	Yes	13.8	5	73.3	No	Wild type
9	74	M	No	Yes	343	0.1	No	82.5	14.2	129	No	Wild type
10	53	M	No	Yes	330	0.5	Yes	22.5	9.4	63.3	No	Wild type
11	51	F	Yes	Yes	1330	0.6	Yes	<5	12.3	*	No	c.451G>A (p.G151R)
12	68	F	No	No	139	<0.1	*	22.3	3.6	21.3	No	Wild type
13	26	F	No	No	500	<0.1	No	17.1	1.7	*	No	c.503T>G (p.L168R)
14	35	F	No	No	287	0.3	No	19.7	4.7	33.3	No	c.451G>C (p.G151R)
15	61	F	No	No	366	<0.1	No	14.9	2.9	58.2	No	Wild type
16	64	M	No	No	521	<0.1	No	27.9	3.7	*	No	c.451G>A (p.G151R)
17	31	M	No	No	353	<0.1	No	29.3	2.2	39.2	No	c.451G>A (p.G151R)
18	61	M	No	No	484	0.2	No	22	1.4	102	No	Wild type
19	41	F	No	No	176	0.2	No	34.3	1.0	*	No	c.451G>A (p.G151R)
20	63	F	No	No	363	<0.1	No	29.5	2.3	30.5	No	c.451G>C (p.G151R)
21	73	F	No	No	260	<0.1	*	12.5	*	23.4	No	Wild type
22	50	M	No	No	426	0.2	No	10.8	2.5	36.2	No	c.451G>A (p.G151R)
23	55	M	No	No	299	0.1	No	28.4	1.8	52	No	c.451G>A (p.G151R)
24	36	F	No	No	542	0.2	No	11.5	5.9	49.6	No	c.503T>G (p.L168R)
25	50	M	No	No	1330	<0.1	No	17.4	29.5	29.5	No	c.451G>A (p.G151R)
26	52	M	No	No	693	0.3	No	44	4.4	132	No	c.451G>A (p.G151R)
27	42	F	No	No	358	0.9	*	15	2.4	*	No	c.503T>G (p.L168R)
28	65	M	No	No	1990	<0.1	No	43.6	3.4	69.6	No	c.451G>C (p.G151R)
29	50	F	No	No	88.9	0.3	No	20.2	1.7	74.8	No	c.451G>A (p.G151R)
30	41	F	No	No	224	0.3	No	44.1	7.4	33.1	No	c.503T>G (p.L168R)
31	32	M	No	No	1212	0.4	No	46	2.5	73.4	No	c.451G>A (p.G151R)
32	50	F	No	No	517	0.4	*	23.8	*	*	No	c.451G>C (p.G151R)
33	46	M	No	No	130	0.1	No	22.3	3.7	99.2	No	c.451G>C (p.G151R)

PRKACA mutation represents a heterozygous mutation of c.617T>G (p.L206R). *KCNJ5* mutation represents a heterozygous mutation of c.451G>C (p.G151R), c.451G>A (p.G151R), or c.503T>G (p.L168R). M, male; F, female. Specific cushingoid signs refer to the guidelines of the Endocrine Society. 1 mg DST, serum cortisol levels in the 1 mg dexamethasone suppression test. Mild hypercortisolism was defined as at least one abnormal result of suppressed plasma ACTH levels below 10 pg/mL, midnight serum cortisol levels above 7.5 μg/dL, or a 1 mg dexamethasone suppression test result > 3.0 μg/dL. 1 mg DST, a 1 mg dexamethasone suppression test result > 3.0 μg/dL is indicated as Yes. * No data were available.

either pure APA or APA co-secreting cortisol.

Ratio of wild-type and mutated PRKACA mRNA levels examined by PCR-RFLP

To evaluate the expression of mutant mRNA, we performed a PCR-RFLP assay on the CPAs with the mutation p.L206R (c.617T>G), namely, patients 1-3 in Table 1. As shown in Fig. 2, the 213-bp band corresponded to the amplified cDNA and the 273-bp band was amplified genomic DNA that included a short intron, 148 bp in length. The complete digestion by the enzyme was confirmed by PCR fragments of the genomic DNA, and no band remained after digestion. The density of the 213-bp fragment after digestion with the BciT130 I restriction enzyme was similar to that of the 162-bp fragment (the ratio of 213-bp /162-bp fragment (101.8 ± 1.4%, n=3)), suggesting that the mutant mRNA c.617T>G may be expressed at a level similar to that of the wild type.

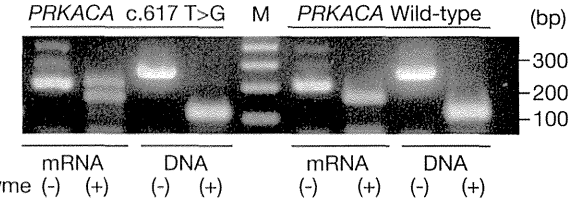

Fig. 2 PCR-RFLP assay of CPAs with c.617T>G, p.L206R
The wild-type fragment had the site digested by the BciT130 I restriction enzyme. The 213-bp PCR product encompassing the 617T>G mutation was digested with BciT130 I, and the fragments were resolved on a 2% agarose gel. The wild-type allele was cut into two fragments of 162- and 52-bp, while the mutated allele remained uncut. Similarly, the wild-type genomic DNA was cut into fragments 127 bp and 147 bp in length. We compared the density of the 213-bp and 162-bp fragments after digestion to evaluate the ratio of the levels of mutated and -wild-type *PRKACA* mRNA. We found that the mutant mRNA was expressed at a level similar to that in the wild-type. Representative data are shown. 'Enzyme' refers to digestion with a restriction enzyme, BciT130 I, and lane M is a molecular marker ladder.

Discussion

In the present study, we identified heterozygosity for an T-to-G transition 617 bp from the translation start site in the *PRKACA* gene (c.617T>G) in 3 of 13 of the patients, which is the same mutation as reported by Beuschlein *et al.*, resulting in a leucine-to-arginine substitution at codon 206 (p.L206R) [10]. Beuschlein *et al.* reported another mutation, c.595_596insCAC, in 1 case of overt Cushing's syndrome [10] . However, we did not find the same mutation in our cases. During the preparation of this manuscript Cao *et al.* and Sato *et al.* reported a higher prevalence (approximately 67% and 52%, respectively) of the same mutation of the *PRKACA* gene in Chinese and Japanese CPAs showing overt Cushing's syndrome [18, 19]. However, we found a similar prevalence of the mutation as that in Western countries. This may be due to differences in the severity of disease or environmental factors, although this requires further study.

Although the term "preclinical" Cushing's syndrome was previously proposed, the term "subclinical" Cushing's syndrome describes this condition more accurately, as it does not imply any assumption about the further development of a clinically overt syndrome [20, 21]. Since the prevalence of overt Cushing's syndrome caused by adrenal adenoma in the general population is markedly lower than the prevalence of subclinical Cushing's syndrome in patients with clinically non-functioning adrenal adenoma, it is rather inappropriate to consider subclinical Cushing's syndrome as an early stage of the development of overt hypercortisonemia [20, 22]. Neither we nor Beuschlein *et al.* found mutations of the *PRKACA* gene in cases that showed subclinical Cushing's syndrome, so these findings further support the evidence that the origin of the tumors showing overt Cushing's syndrome differs from that of tumors showing subclinical Cushing's syndrome [10]. Although Sato *et al.* found the mutation in one case out of 9 tumors showing subclinical Cushing's syndrome, this may be due to the difference of the definition of subclinical Cushing's syndrome used for the diagnosis [19]. Sato *et al.* diagnosed patients who had an incidentally discovered adrenocortical adenoma and no typical symptoms or signs of Cushing's syndrome.

We previously reported that some APAs showing clear autonomous cortisol secretion had mutation of the *KCNJ5* gene, suggesting that these tumors had the same features as APAs not co-secreting cortisol [13]. In a previous study, we defined the patients with all of the following criteria as having "clear cortisol secretion": 1) low ACTH level <10 pg/mL, 2) suppressed accumulation of adosterol in scintigraphy on the intact side of the adrenal gland, and 3) post-adrenal insufficiency [13]. In the present study, we used serum morning cortisol level not being suppressed below 3 μg/dL

by 1 mg DST as a parameter of mild hypercortisolemia, but we did not find any *PRKACA* mutations in these tumors, even without *KCNJ5* mutations. Furthermore, some APAs co-secreting cortisol had *KCNJ5* mutation, suggesting that these tumors seem to be close to the features of APAs, rather than CPAs.

We established a simple assay to detect the mutation hotspot of the *PRKACA* gene using PCR-RFLP. The mutation causes loss of the enzyme site for digestion by the BciT130 I restriction enzyme. Although the sequence spike of the mutated allele seems to be lower than that of the wild-type allele in the present study and the same phenomenon has been described in reports by Beuschlein *et al.* [10] and Cao *et al.* [18], the results demonstrate that the mutated allele was expressed as was the wild-type allele.

Cao *et al.* also identified other somatic mutations co-localizing with PRKACA mutations in CPAs, including activating CTNNB1 mutations and an APC truncating mutation, activating GNAS (stimulatory G-protein α subunit), mutations in cancer-related genes such as *ARID1A* and *STAT3*, and recurrently mutated GPR98 [18]. Sato *et al.* also found a GNAS mutation in some CPAs [19]. In addition, Goh *et al.* reported that some CPAs had many somatic copy number variants (CNVs), with frequent deletion of *CDC42* and *CDKN2A*, amplification of 5q31.2, mutations of TP53 or RB1, CTNNB1 (b-catenin), or GNAS [11]. In the present study, we did not find PRKACA mutations in any of the cases of subclinical Cushing's syndrome and APAs associated with cortisol. Therefore, the other mutations mentioned above may be involved in the pathophysiology of cortisol secretion in these tumors.

Acknowledgements

This study were supported in part by a Health and Labor Sciences Grant for Research on Measures for Intractable Disease (M.Y.) and KAKENHI (Grant-in-Aid for Reseach Activity Start-up 25893026) (Y.N.).

We thank all the medical and co-medical staff as well as graduate students involved in the patient care.

Disclosure Summary

All authors have nothing to disclose.

References

1. Nieman L, Biller B, Findling J, Newell-Price J, Savage M, et al. (2008) The diagnosis of Cushing's syndrome: an Endocrine Society Clinical Practice Guideline. *J Clin Endocrinol Metab* 93: 1526-1540.
2. Newell-Price J, Bertagna X, Grossman AB, Nieman LK (2006) Cushing's syndrome. *Lancet* 367: 1605-1617.
3. Rossi R, Tauchmanova L, Luciano A, Di Martino M, Battista C, et al. (2000) Subclinical Cushing's syndrome in patients with adrenal incidentaloma: clinical and biochemical features. *J Clin Endocrinol Metab* 85: 1440-1448.
4. Terzolo M, Reimondo G, Bovio S, Angeli A (2004) Subclinical Cushing's syndrome. *Pituitary* 7: 217-223.
5. Grumbach M, Biller B, Braunstein G, Campbell K, Carney J, et al. (2003) Management of the clinically inapparent adrenal mass ("incidentaloma"). *Ann Intern Med* 138: 424-429.
6. Tsagarakis S, Vassiliadi D, Thalassinos N (2006) Endogenous subclinical hypercortisolism: Diagnostic uncertainties and clinical implications. *J Endocrinol Invest* 29: 471-482.
7. Nakajima Y, Yamada M, Taguchi R, Satoh T, Hashimoto K, et al. (2011) Cardiovascular complications of patients with aldosteronism associated with autonomous cortisol secretion. *J Clin Endocrinol Metab* 96: 2512-2518.
8. Adachi J, Hirai Y, Terui K, Nakano T, Fukuda Y, et al. (2003) A report of 7 cases of adrenal tumors secreting both cortisol and aldosterone. *Intern Med* 42: 714-718.
9. Späth M, Korovkin S, Antke C, Anlauf M, Willenberg HS (2011) Aldosterone- and cortisol-co-secreting adrenal tumors: the lost subtype of primary aldosteronism. *Eur J Endocrinol* 164: 447-455.
10. Beuschlein F, Fassnacht M, Assié G, Calebiro D, Stratakis CA, et al. (2014) Constitutive activation of PKA catalytic subunit in adrenal Cushing's syndrome. *N Engl J Med* 370: 1019-1028.
11. Goh G, Scholl UI, Healy JM, Choi M, Prasad ML, et al. (2014) Recurrent activating mutation in PRKACA in cortisol-producing adrenal tumors. *Nat Genet* 46: 613-617.
12. Taguchi R, Yamada M, Nakajima Y, Satoh T, Hashimoto K, et al. (2012) Expression and Mutations of KCNJ5 mRNA in Japanese Patients with Aldosterone-Producing Adenomas. *J Clin Endocrinol Metab* 97: 1311-1319.
13. Yamada M, Nakajima Y, Taguchi R, Okamura T, Ishii S, et al. (2012) KCNJ5 mutations in aldosterone- and cortisol-co-secreting adrenal adenomas. *Endocr J* 59: 735-741.
14. Mulatero P, Monticone S, Rainey WE, Veglio F, Williams TA (2013) Role of KCNJ5 in familial and spo-

radic primary aldosteronism. *Nat Rev Endocrinol* 9: 104-112.
15. Funder J, Carey R, Fardella C, Gomez-Sanchez C, Mantero F, et al. (2008) Case Detection, Diagnosis, and Treatment of Patients with Primary Aldosteronism: An Endocrine Society Clinical Practice Guideline. *J Clin Endocrinol Metab* 93: 3266-3281.
16. Hiraishi K, Yoshimoto T, Tsuchiya K, Minami I, Doi M, et al. (2011) Clinicopathological features of primary aldosteronism associated with subclinical Cushing's syndrome. *Endocr J* 58: 543-551.
17. Ishida E, Yamada M, Horiguchi K, Taguchi R, Ozawa A, et al. (2011) Attenuated expression of menin and p27 (Kip1) in an aggressive case of multiple endocrine neoplasia type 1 (MEN1) associated with an atypical prolactinoma and a malignant pancreatic endocrine tumor. *Endocr J* 58: 287-296.
18. Cao Y, He M, Gao Z, Peng Y, Li Y, et al. (2014) Activating Hotspot L205R Mutation in PRKACA and Adrenal Cushing's Syndrome. *Science* 344: 913-917.
19. Sato Y, Maekawa S, Ishii R, Sanada M, Morikawa T, et al. (2014) Recurrent somatic mutations underlie corticotropin-independent Cushing's syndrome. *Science* 344: 917-920.
20. Chiodini I (2011) Clinical review: Diagnosis and treatment of subclinical hypercortisolism. *J Clin Endocrinol Metab* 96: 1223-1236.
21. Barzon L, Sonino N, Fallo F, Palu G, Boscaro M (2003) Prevalence and natural history of adrenal incidentalomas. *Eur J Endocrinol* 149: 273-285.
22. Mantero F, Terzolo M, Arnaldi G, Osella G, Masini A, et al. (2000) A survey on adrenal incidentaloma in Italy. Study Group on Adrenal Tumors of the Italian Society of Endocrinology. *J Clin Endocrinol Metab* 85: 637-644.

Biochemical and Biophysical Research Communications 451 (2014) 24–29

Contents lists available at ScienceDirect

Biochemical and Biophysical Research Communications

journal homepage: www.elsevier.com/locate/ybbrc

Coordinated regulation of transcription and alternative splicing by the thyroid hormone receptor and its associating coregulators

Tetsurou Satoh [a,*], Akiko Katano-Toki [a], Takuya Tomaru [a], Satoshi Yoshino [a], Takahiro Ishizuka [a], Kazuhiko Horiguchi [a], Yasuyo Nakajima [a], Sumiyasu Ishii [a], Atsushi Ozawa [a], Nobuyuki Shibusawa [a], Koshi Hashimoto [a], Masatomo Mori [b], Masanobu Yamada [a]

[a] Department of Medicine and Molecular Science, Gunma University Graduate School of Medicine, Maebashi, Japan
[b] Kitakanto Molecular Novel Research Institute for Obesity and Metabolism, Midori, Japan

ARTICLE INFO

Article history:
Received 1 July 2014
Available online 11 July 2014

Keywords:
Thyroid hormone receptor
Transcription
Alternative splicing
Thyroid hormone receptor-associated protein
150-kDa
Polypyrimidine tract-binding protein-associated splicing factor

ABSTRACT

Emerging evidence has indicated that the transcription and processing of precursor mRNA (pre-mRNA) are functionally coupled to modulate gene expression. In collaboration with coregulators, several steroid hormone receptors have previously been shown to directly affect alternative pre-mRNA splicing coupled to hormone-induced gene transcription; however, the roles of the thyroid hormone receptor (TR) and its coregulators in alternative splicing coordinated with transcription remain unknown. In the present study, we constructed a luciferase reporter and CD44 alternative splicing (AS) minigene driven by a minimal promoter carrying 2 copies of the palindromic thyroid hormone-response element. We then examined whether TR could modulate pre-mRNA processing coupled to triiodothyronine (T3)-induced gene transcription using luciferase reporter and splicing minigene assays in HeLa cells. In the presence of cotransfected TRβ1, T3 increased luciferase activities along with the inclusion of the CD44 variable exons 4 and 5 in a dose- and time-dependent manner. In contrast, cotransfected TRβ1 did not affect the exon-inclusion of the CD44 minigene driven by the cytomegalovirus promoter. T3-induced two-exon inclusion was significantly increased by the cotransfection of the TR-associated protein, 150-kDa, a subunit of the TRAP/Mediator complex that has recently been shown to function as a splicing factor. In contrast, T3-induced two-exon inclusion was significantly decreased by cotransfection of the polypyrimidine tract-binding protein-associated splicing factor, which was previously shown to function as a corepressor of TR. These results demonstrated that liganded TR in cooperation with its associating cofactors could modulate alternative pre-mRNA splicing coupled to gene transcription.

1. Introduction

Gene transcription is orchestrated by the coordinated efforts of ATP-dependent chromatin remodeling, histone modification, transcription initiation, elongation, and termination, and RNA processing [1,2]. Although each of these biochemical reactions is accomplished by diverse protein complexes, communication between transcription factors and RNA splicing factors indicates co-transcriptional RNA splicing, which is performed by one general gene expression machine [1,2]. Alternative pre-mRNA splicing is regulated temporally and spatially and is a major source of protein diversity for higher eukaryotes. More than 90% of genes in humans have been estimated to generate multiple protein isoforms derived from alternative splicing (AS) [3]. Aberrant pre-mRNA splicing caused by mutations in consensus splice regulatory sequences and functional mutations in splicing factors have been reported to play pathogenic roles in various human disorders including endocrine and metabolic diseases, cancers, hematological malignancies, and neurodegenerative diseases [4–6]. Therefore, elucidating the mechanisms underlying pre-mRNA processing in more detail is important for understanding the pathogenesis of human diseases caused by deranged RNA splicing and the development of new treatment strategies.

Nuclear hormone receptors (NRs) are transcription factors that bind hormone response elements located in the responsible genomic regions of target genes and regulate gene transcription in ligand-dependent and -independent manners [7,8]. Previous findings confirmed that NRs dynamically interacted with diverse classes of transcriptional coregulators (TCRs) to regulate target

* Corresponding author. Address: Department of Medicine and Molecular Science Gunma University Graduate School of Medicine, 3-39-15 Showa-machi, Maebashi 371-8511, Japan. Fax: +81 27 220 8136.
E-mail address: tsato@gunma-u.ac.jp (T. Satoh).

http://dx.doi.org/10.1016/j.bbrc.2014.07.029
0006-291X/

gene transcription [9–11]. These TCRs possess intrinsic and associated enzymatic activities and modulate the recruitment of RNA polymerase II (pol II) to the transcription start site mainly by the ATP-dependent remodeling of chromatin structures and epigenetic modification of histone tails [9–11]. Emerging evidence has indicated that several NRs including the peroxisome proliferator-activated receptor (PPAR)γ, estrogen receptor (ER), progesterone receptor (PR), and androgen receptor (AR) may coordinate hormone-induced gene transcription with pre-mRNA processing in collaboration with specific TCRs and/or splicing factors [12–16]. Triiodothyronine (T3) activates the thyroid hormone receptor (TR), which binds to the thyroid hormone-response element (TRE) in both the absence and presence of a ligand [17], and has previously been shown to modulate the AS of beta-amyloid and TRα genes expressed in cultured cells [18,19]. The TR-associated protein, 150-kDa (TRAP150) (also known as TR-associated protein3, THRAP3), was originally isolated as a subunit of the TRAP/Mediator complex, which can be recruited to liganded TR and facilitate the recruitment of pol II to initiate transcription [20], and has recently been shown to play a role in pre-mRNA splicing [21–23]. In addition, the polypyrimidine tract-binding protein (PTB)-associated splicing factor (PSF) (also known as splicing factor proline/glutamine-rich, SFPQ), initially isolated as a protein that interacted with PTB [24] and was recently shown to associate with the DBIRD complex, which integrates AS and pol II transcript elongation [25], has previously been reported to function as a transcriptional corepressor of NRs including TR [26–28]. Taken together, these findings suggest that TR could regulate not only gene transcription, but also pre-mRNA processing in coordination with TRAP150 and/or PSF. However, the co-transcriptional regulation of AS by TR has not yet been examined.

In the present study, we constructed a luciferase reporter vector and CD44 AS minigene driven by the identical minimal promoter carrying the palindromic TRE and examined whether liganded TR could modulate the alternative splicing of CD44 variable exons coupled with gene transcription in collaboration with TRAP150 and/or PSF.

2. Materials and methods

2.1. Cell cultures

HeLa cells were were split 24 h before transfection and cultured in DMEM containing resin–charcoal double stripped 10% fetal bovine serum during the T3 treatment as previously described [29,30].

2.2. Plasmids

The expression vectors of human TRβ1 (pKCR$_2$-hTRβ1), TRAP150 (pSV-SPORT-hTRAP150), and PSF (pCS3+MT-hPSF) were described previously [29–31]. The pGL4.23[*luc2*/minP] vector containing firefly luciferase (*Luc2*) cDNA under the control of a minimal promoter containing a TATAA box was obtained from Promega Corporation (Madison, MI). The DNA fragment containing two copies of palindromic (PAL) TRE (AGGTCATGACCT) was amplified by PCR using a primer pair as described [32] and a 2 × PAL-thymidine kinase luciferase vector [32] as a template. The PCR amplified fragment was ligated into the pGEM-T Easy vector (Promega Corporation) to yield pGEM-T Easy-PAL, and the *Eco*RI digested fragment was then ligated into the *Eco*RI site of pGEM11Zf (Promega Corporation) to yield pGEM11Zf-PAL. The DNA fragment obtained by the *Sac*I digestion of pGEM11Zf-PAL was finally ligated into the *Sac*I site of pGL4.23[*luc2*/minP] (pGL4.23 PAL-Luc). The cytomegalovirus (CMV) promoter-driven CD44 minigene (CMV-CD44) was described previously [13]. The CMV-CD44 minigene contains a genomic DNA fragment including variable exons 4 (v4) and 5 (v5) of the CD44 gene along with their surrounding introns in the intron between exon 1 and exon 2 of the human β globin gene (CD44 minigene cassette) [33]. *Luc2* cDNA in pGL4.23 PAL-Luc or pGL4.23[*luc2*/minP] was excised by *Nco*I and *Xba*I digestion and replaced by the PCR-amplified CD44 minigene cassette to obtain pGL4.23 PAL-CD44 or pGL4.23 minP-CD44, respectively. The proper construction of pGL4.23 PAL-Luc, pGL4.23 PAL-CD44, and pGL4.23 minP-CD44 was verified by nucleotide sequencing.

2.3. Lipofection, RNA isolation, and RT-PCR

Plasmids were transfected into HeLa cells in 60-mm culture dishes using Lipofectamine 2000 reagent (Invitrogen, Life Technology Corporation, Tokyo, Japan). The total amounts of the transfected plasmids were adjusted using empty expression vectors. After incubation with T3 (Sigma Aldrich Japan, Osaka, Japan), total RNA was isolated using Isogen (Nippon Gene Co., Ltd., Tokyo, Japan). AS minigene assays were performed according a previously described protocol [13] with modifications. Briefly, 5 μg of total RNA was treated with RQ1 DNase (Promega Corporation) at 37 °C for 30 min followed by the inactivation of DNase with the addition of the Stop buffer (Promega Corporation) at 65 °C for 10 min. DNase-treated RNA was denatured for 5 min at 65 °C and annealed with an antisense primer complementary to the sequence in exon 2 of the human β globin gene (HBB-AS: 5′-CCATAACAGCATCAGGAGTG-3′). First strand cDNA was synthesized using Superscript III reverse transcriptase (Invitrogen) at 50 °C for 30 min according to the manufacturer's protocol. One microliter of the cDNA sample was subjected to PCR in a total volume of 50 μl using AmpliTaq DNA polymerase (Applied Biosystems by Roche Molecular Systems, Inc., Branchburg, NJ) and a PCR primer pair; sense 5′-ACGTGGATGAAGTTGGTGGT-3′, which was complementary to exon 1 of HBB (HBB-S), and HBB-AS. The PCR conditions used were denaturing at 94 °C for 30 s, annealing at 60 °C for 45 s, and extension at 72 °C for 1 min for 35 cycles. The PCR products were subjected to electrophoresis in agarose gels containing ethidium bromide, and band intensities were quantitated using an image analyzer. The proper amplification of AS products was verified by nucleotide sequencing.

2.4. Luciferase assay

HeLa cells were split into 6-well plates and pGL4.23PAL-Luc along with TR expression vectors or an empty expression vector were transfected using a calcium phosphate precipitation method. The luciferase assay was performed as described [29,30].

2.5. Statistical analysis

Statistical analysis was performed using ANOVA, followed by Turkey's multiple comparison tests. Significance was set at $p < 0.05$.

3. Results

To examine whether TR could modulate transcription-coupled alternative pre-mRNA splicing, we constructed a luciferase reporter vector and CD44 AS minigene driven by the identical minimal promoter carrying PAL-TRE (Fig. 1). Three alternatively spliced RNA products could theoretically be generated at different levels from this CD44 minigene cassette that included two exons (v4 and v5), one exon (v4 or v5), or no exon in the context of the

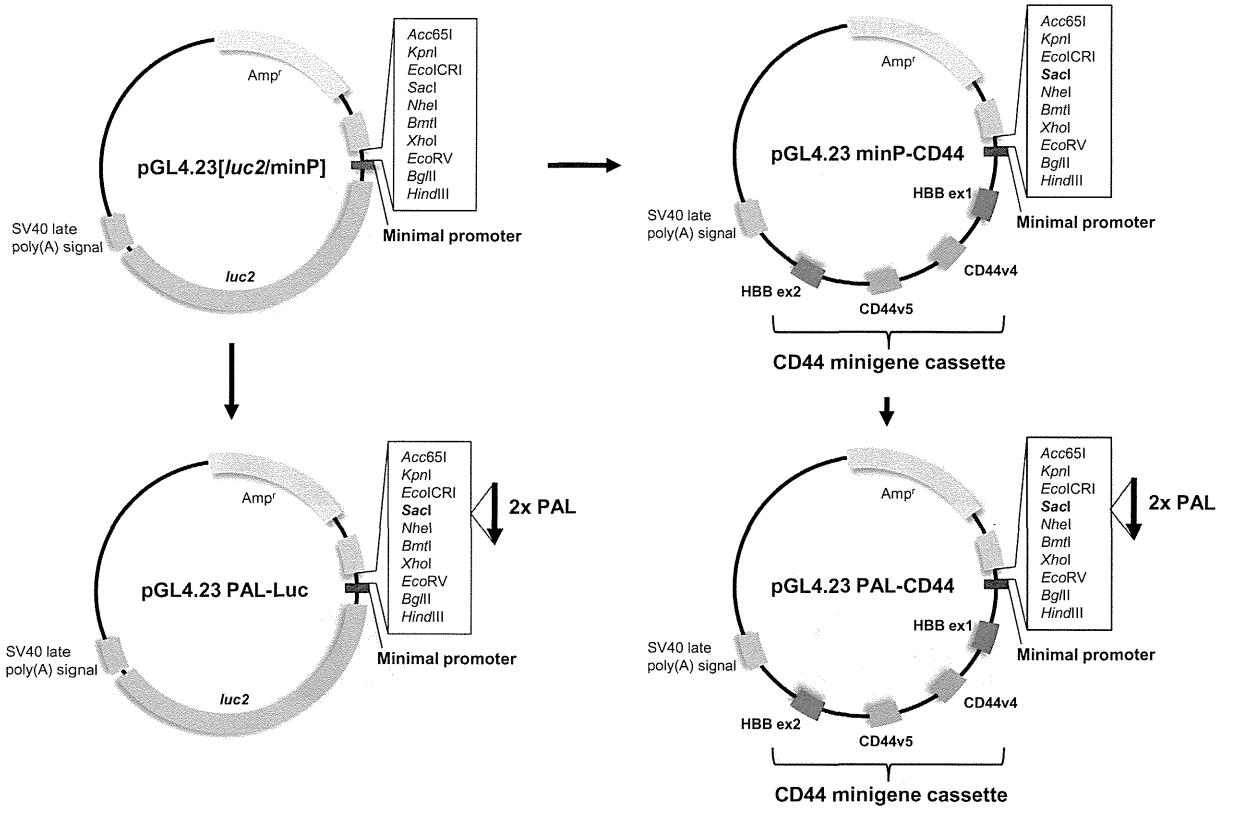

Fig. 1. Construction of a luciferase reporter vector and AS CD44 minigene driven by a minimal promoter carrying the palindromic TRE (PAL). pGL4.23 PAL-Luc, pGL4.23 minP-CD44, and pGL4.23 PAL-CD44 were constructed as described in the Section 2. The positions of multiple cloning sites (an open box), CD44 minigene cassette, the ampicillin-resistant gene (Amp^r), and simian virus (SV) 40 late poly (A) signal are indicated.

driving promoter or transfected cultured cells [13,15,16]. We then cotransfected PAL-Luc or PAL-CD44 with the TRβ1 expression vector into HeLa cells and luciferase and minigene assays were performed in parallel 24 h after incubations with increased concentrations of T3. In the agarose gel electrophoresis of RT-PCR products, only one-exon (v5)-included CD44 RNA was observed in the absence of T3, whereas T3 significantly increased RNA including v4 and v5 in a dose-dependent manner (Fig. 2B). In parallel with the increase of the two-exon inclusion by T3, T3 significantly stimulated the promoter activity of PAL-Luc in a dose-dependent manner (Fig. 2A). T3 also increased the inclusion of two variable exons in a time-dependent manner, and this appeared to be in parallel with the promoter activities of PAL-Luc stimulated by T3 (Fig. 2D and C). These results indicated that T3 could coordinately regulate the transcription of PAL-Luc and AS decision of PAL-CD44 minigene in a dose- and time-dependent manner in the presence of cotransfected TR.

T3 may alter the expression levels of cellular splicing factors, thereby increasing the two-exon included transcript generated from PAL-CD44; therefore, we evaluated whether the AS of the CMV-CD44 minigene lacking functional TREs could be influenced by cotransfected TR. As shown in Supplementary Fig. 1, two-exon and 0-exon included RNA was detected from the CMV-CD44 minigene (the upper panel), whereas cotransfected TRβ1 did not increase the amounts of two-exon included RNA in the presence of T3 (the lower panel). These results suggested that the T3-induced increase in two-exon included CD44 transcripts from PAL-CD44 may be mediated by TRE-bound TR. In addition, different promoters (i.e. PAL vs. CMV) could alter the AS decision of the CD44 minigene.

To evaluate whether these dual-functional TCRs of TR affected T3-induced gene activation as well as AS decisions, the expression vectors for TRAP150 or PSF in the absence or presence of TR was cotransfected with the PAL-Luc or PAL-CD44 minigene, and luciferase activities and splicing reactions were examined in the absence or presence of T3. As shown in Fig. 3A, cotransfected TRAP150 did not stimulate TR-mediated gene transcription in luciferase assays. In contrast, cotransfected TRAP150, but not HELZ2, a DNA/RNA helicase that could interact with TRAP150 [28], significantly increased two-exon inclusion in the presence of liganded TR (Fig. 3B). Consistent with the findings of a previous study [26], the cotransfection of PSF significantly reduced TR-mediated activation of PAL-Luc (Fig. 4A). In addition, cotransfected PSF significantly decreased the two-exon inclusion of the CD44 minigene in the presence of liganded TR (Fig. 4B). In contrast, the two-exon inclusion of the CD44 minigene driven by the CMV promoter was not increased by cotransfected TRAP150, but was paradoxically increased by cotransfected PSF via an unknown mechanism (Supplementary Fig. 2). Taken together, these results indicated that TRAP150 and PSF, two known TCRs of TR, could modulate the co-transcriptional AS of the CD44 minigene mediated by TRE-bound TR.

4. Discussion

It is now increasingly evident that mRNA transcription and processing events are coordinately regulated in the nucleus [1,2]. This coordination was shown to be mediated largely by the C-terminal domain (CTD) of the largest subunit of pol II, which is responsible for the recruitment of splicing factors to transcription sites *in vivo* [1,2]. The initiation form of pol II contains hypophosphorylated CTD (pol IIa), whereas the elongation form of pol II contains a CTD that is hyperphosphorylated (pol IIo) by several kinases [1,2]. This transition of the phosphorylated status from pol IIa to pol IIo is thought to result in the recruitment of some pre-mRNA